KUNS 1226
November, 1993

Energy Properties of Strange Quark Matter Studied in Consitituent Quark Model

MITSURU ISHII, RYOZO TAMAGAKI AND AKIHIRO TOHSAKI*

Department of Physics, Kyoto University, Kyoto 606-01

and

** Department of Fine Materials Engineering, Shinshu University, Ueda 386*

ABSTRACT

We study energy properties of strange quark matter (SQM) in an approach based on the constituent quark model. In treating the infinite matter, SQM is modeled on a cubic lattice composed of the 1s-closed shell (Q_s) clusters, by extending a cluster-theoretical approach previously made for finite strange quark systems of Q_s-clusters. The energy per baryon of this SQM ($\mathcal{E}_{\rm SQM}$) monotonously increases as the inter-Q_s distance decreases (the density of Q_s-clusters as well as the average baryon number density increases). This means that Q_s-clusters do not fuse to the Fermi-gas like SQM and favor to be far apart from each other. The mechanism causing such tendency is the following; the repulsive contributions to the inter-Q_s energy coming from the kinetic energy and the color magnetic interaction overwhelm the attractive ones from the color electric interaction and the contributions from a confinement potential play no essential role. The energy of SQM per baryon can never be less than that of a single Q_s which is higher by about 400 $\sim$ 500 MeV than the nucleon mass. Therefore the appearance of the absolutely stable SQM is unlikely in this model. Saturation property of SQM and surface effects are also discussed.

1. Introduction and summary

Strange quark matter (abbreviated to SQM) has attracted much attention, since Witten[1] conjectured a possible existence of the absolutely stable SQM, whose energy per baryon ($\mathcal{E}_{\rm SQM} \equiv E_{\rm SQM}/N_b, N_b$ being the baryon number) is lower than that of the nucleus $\mathcal{E}_N$, namely, $\mathcal{E}_N \simeq 930$ MeV for ^{56}Fe and $\mathcal{E}_N \simeq 923$ MeV for nuclear matter. Many works on SQM have been made by focusing on the phenomena this possibility may bring about.[2] On the other hand, there are fundamental questions on SQM as to whether or not the notion of the absolutely stable SQM is free from inconsistency from the viewpoint of many-body theory. This paper is concerned with the latter point.

In previous works, two of the authors (M.I. and R. T.) studied the saturation property of SQM in two QCD-motivated effective models, namely, in the constituent quark model[3] and in the bag model,[4] by taking into account the one-gluon exchange effect on equal footing throughout all the baryon numbers (N_b) of the systems under consideration.* The principal result obtained commonly in these two approaches is that $\mathcal{E}_{\rm SQM}$ is no smaller than that of the 1s-closed shell ($N_b = 6$), as shown in Fig.1.

In a bag-model approach (BMA),[4] calculations were made for the infinite matter as for the finite systems of the closed-shell states up to $N_b = 24$ ($N_b = 6$, 18 and 24). Three pairs of lines (I, II and III) connecting the same marks shown in Fig.1 are the results obtained with three sets of the bag-model parameters, which cover typical baryon densities of the systems ($\rho_b \gtrsim 15\rho_N, (6 \sim 7)\rho_N$ and $(1.4 \sim 1.6)\rho_N$, respectively, $\rho_N \simeq 0.17$ fm^{-3} being the nuclear density). On the right of the figure, $\mathcal{E}_{\rm SQM}$ of the infinite matter are shown. The lines with the filled (open) marks show the energy per baryon of the systems with equal numbers of $u, d, s(u, d)$. For the case III giving rise to $\mathcal{E}_{\rm SQM} \simeq m_N - 50$ MeV (m_N being the nucleon mass) in the limit $N_b \to \infty$, [5] the energy per baryon of the u, d system for finite $N_b \lesssim 100$ is even lower than those of finite nuclei, and also inconsistent with the baryon data. For the case I (II), whose model parameters reproduce the baryon (hadron) spectra under some supplementary considerations, we have a steeply (moderately) increasing function for $\mathcal{E}_{\rm SQM}$ beyond $N_b = 6$.

In a quark cluster-model approach (CMA),[3] we utilized a framework of nuclear cluster theory, taking the 1s-closed shell state as a building-block (cluster), which is abbreviated to

* In this paper, ref.3) made in a cluster-model approach and ref.4) in a bag-model approach are refered to as CMA and BMA, respectively.

Q_s. The Q_s cluster is considered as a hypothetical subunit composed of the equal number of u, d, s, which serves for studying whether the notion of the absolutely stable SQM is reasonably acceptable or not. The aggregates of Q_s-clusters can be smoothly transformed to multi-quark systems with a Fermi-gas like feature, when they overlap largely. In Fig.1, $\mathcal{E}_{\rm SQM}$ up to four Q_s-cluster systems (N_b=6, 12, 18, 24) are shown by crosses (diamonds) for a linear (quadratic) confinement potential. For N_b=24, the system tends to the 1p-closed shell state when four Q_s fully overlap in the terahedral configuration. For a variety of spatial configurations of Q_s, the energy of the multi-Q_s systems increases when Q_s-clusters approach each other. This means that the multi-Q_s systems have the lowest state when they are well separated, that is, $\mathcal{E}_{\rm SQM} = E(Q_s)/6$, $E(Q_s)$ being the energy of a single Q_s. This property is shown by two dotted horizontal lines in Fig.1.

The cluster-theoretical approach has the advantage, which provides us with clear understanding on the contents of $\mathcal{E}_{\rm SQM}$ in terms of the contribution of a single Q_s and the change from it due to the inter-Q_s contributions. Also it is powerful in treating the quark many-body system, where all the interaction effects come from the exchange terms.

The infinite Q_s matter was not studied in CMA, although some reasoning was discussed there concerning the possibility that the feature mentioned above persists up to larger Q_s systems. This reasoning has been based on the observations of the contributions to $\mathcal{E}_{\rm SQM}$ from the respective terms as shown below.

	Q_s- internal	Inter - Q_s (mutual)
kinetic energy	largely positive	strongly repulsive
color electric interaction (CEI)	strongly attractive	attractive
color magnetic interaction (CMI)	strongly repulsive	repulsive
confinement potential	strongly repulsive	weakly attractive or vanishing

The mutual interaction among Q_s-clusters lacks a strong attraction that overwhelms the strong repulsive effect coming from the kinetic energy increase due to overlapping as Q_s-clusters approach each other. This is mainly because of the color neutrality of Q_s, which makes all the direct terms of the interaction vanishing and only the exchange terms responsible for the mutual interaction.

In this paper we aim to show that the above-mentioned feature is real also in the infinite Q_s-matter, by calculating the energies of Q_s- systems for $N_b \to \infty$. We consider SQM composed of Q_s located on a cubic lattice with the nearest-neighbor distance d, which we

call the Q_s-matter. When d is less than the size of Q_s so that Q_s-clusters considerably overlap, the Q_s-matter has a feature similar to a correlated Fermi gas of SQM. For this lattice configuration we can apply a new calculational scheme, which one of the authors (A.T.) has recently developed in studying the nuclear matter of α-clusters.[6] It enalbes us to calculate three-dimensional lattice problems with a large number of Q_s-clusters (essentially with infinite number), by the use of a direct product form consisting of the quantities constructed in one-dimensional lattice chain.

Results of the present calculations show that the infinite Q_s-matter has the lowest energy in the limit where all the Q_s are well separated. In Fig.1, therefore we can put the marks (the cross and the diamond) on the extension of the dotted horizontal lines at the right end ($N_b \to \infty$). When the inter-Q_s distance d decreases, $\mathcal{E}_{\rm SQM}$ necessarily increase from the single-$Q_s$value: For example, if we take d so as to give the average baryon density $\bar{\rho}_b = 6\,\rho_N$, $\mathcal{E}_{\rm SQM}$ rise as indicated by the arrows at the right end in Fig.1. We have also made calculations for several finite lattices. We find that, for a given average baryon density, the energies of Q_s-systems per baryon are an increasing function of N_b and the saturation of energy takes place essentially at $N_b = 5^3 \times 6$ for $d \gtrsim 2.1$ fm and at $N_b = 7^3 \times 6$ for $d \simeq 1.8$ fm. Even if the size of Q_s is varied from its optimum value, we can not obtain energy gain enough to overcome the increase of the internal energy of Q_s.

Combining the results of this paper with those of the previous papers,[3),4)] we can say that the energies per baryon of strange quark systems with the equal number of u, d, s can never be less than that of a single Q_s for $N_b > 6$ and persists to be much higher than the nucleon mass. This implies that the absolutely stable strange quark matter is unlikely, as far as the basic input parameters introduced in the adopted models do not alter with variation of baryon number.

We can extract the surface energy from the difference between the energy of the Q_s-cluster on the surface site of the lattice and that of the Q_s-cluster located on the interior site. The negative surface energy results, and this corresponds to the aspect mentioned above, that is, the Q_s-matter has the lowest energy when the Q_s-clusters are well separated.

This paper is organized as follows. In the next section, we recapitulate the model wavefunction, the model Hamiltonian and the basic expressions, which were used in CMA. In §3, we give the computational procedure which enalbes us to calculate the energy of the Q_s-matter. Calculated results for the infinite matter are shown and discussed in §4. Saturation property and surface effects are calculated and discussed in §5. The final section is for

remarks and for comparison with the results obtained previously.

2. Energy expressions for strange quark matter composed of Q_s-clusters

The model wavefunction employed here is the same as in CMA. Difference lies in the following points: Now the number of Q_s-clusters (N_Q) is very large but their configuration is restricted to that of the simple rectangular parallelepiped lattice, while in CMA N_Q is limited but a variety of geometrical configurations of Q_s-clusters have been considered.

The single-particle wavefunction of the quark is taken to be of the $1s$-harmonic oscillator form around each cluster center $\mathbf{R}_\mu (\mu = 1, 2, \cdots, N_Q)$

$$\begin{aligned}\varphi_\alpha(i) &= (b^6\pi^3)^{-1/4} \exp\left\{-(\mathbf{r}-\mathbf{R}_\mu)^2/2b^2\right\} \chi_a(i) \\ &\equiv \phi_\mu(\mathbf{r}_i)\chi_a(i) \quad , \end{aligned} \tag{2.1}$$

where α denotes $\{\mathbf{R}_\mu, a\}$, $\chi_a(i)$ the wavefunction of the internal degrees of freedom (spin, flavor and color), and b the spatial size (average radius) of Q_s. We hereafter specify individual quarks by $i, j, \cdots$, total quantum numbers by $\alpha, \beta, \cdots$, spatial configurations of Q_s-clusters by $\mu, \nu, \cdots$ and internal quantum numbers by $a, b, \cdots$. As in refs.3) and 6) , we adopt a total wavefunction in the generator coordinate scheme well-known in nuclear cluster theory:[7]

$$\Phi(1, \cdots, N_q) = \frac{1}{\sqrt{N_q! det\left\{B_{\alpha\beta}\right\}}} \mathcal{A}\left\{\varphi_\alpha(1)\varphi_\beta(2)\cdots\varphi_\gamma(N_q)\right\} \quad , \tag{2.2}$$

where $N_q = 18\ N_Q$ is the total number of quarks and $\mathcal{A}$ means the antisymmetrization. $B_{\alpha\beta}$ are the overlap matrix elements being orthogonal with respect to the internal degrees of freedom:

$$B_{\alpha\beta} \equiv < \varphi_\alpha \mid \varphi_\beta > = B_{\mu\nu}\delta_{ab} \quad . \tag{2.3}$$

In this scheme, it is essential to get the inverse matrix of $\mathbf{B} \equiv \left\{B_{\mu\nu}\right\}$ in a desired accuracy for a large number of Q_s-clusters, where $B^{-1}_{\alpha\beta} = \delta_{ab}B^{-1}_{\mu\nu}$. Once the inverse matrix $\mathbf{B}^{-1} \equiv \left\{B^{-1}_{\mu\nu}\right\}$ is obtained, it is straightforward to calculate the energy of Q_s-systems.

We adopt the same Hamiltonian given in CMA.* Then the energy expectation value $E(\mathbf{R}_1, \mathbf{R}_2, \cdots, \mathbf{R}_{N_Q}; b)$ is written as follows:

$$\begin{aligned} E(\mathbf{R}_1, \mathbf{R}_2, \cdots, \mathbf{R}_{N_Q}; b) &= < \Phi \mid H \mid \Phi > = < \Phi \mid T \mid \Phi > + < \Phi \mid V \mid \Phi > \quad , \\ < \Phi \mid T \mid \Phi > &= 18 \sum_{\mu\nu} < \phi_\mu \mid t \mid \phi_\nu > B^{-1}_{\mu\nu} \quad , \\ < \Phi \mid V \mid \Phi > &= \sum_{I=\lambda,\lambda\sigma} \left\{ \frac{1}{2} \sum_{\mu\nu\sigma\rho} < \phi_\mu\phi_\nu \mid v^{(I)} \mid \phi_\sigma\phi_\rho > \right. \\ &\qquad \left. \times \left(X^{(I)}_d B^{-1}_{\sigma\mu} B^{-1}_{\rho\nu} + X^{(I)}_e B^{-1}_{\rho\mu} B^{-1}_{\sigma\nu}\right) \right\} \quad . \end{aligned} \tag{2.4}$$

Energy per baryon $\mathcal{E}_{\rm SQM} = E/N_b$ is given as

$$\mathcal{E}_{\rm SQM} = E(\mathbf{R}_1, \mathbf{R}_2 \cdots, \mathbf{R}_{N_Q})/6N_Q \quad , \tag{2.5}$$

because of $N_b = 6N_Q$ in this model. In these expressions, t means the kinetic energy operator of a single quark, $t_i = m_i + \mathbf{p}_i^2/2\bar{m}$ with $\bar{m}$= 372 MeV (an averaged one for flavor) and I denotes the types of interaction used. The $I = \lambda$ term has the color SU_3 generator $\underline{\lambda}_i \cdot \underline{\lambda}_j$ and consists of the confinement potential, $v_{\rm conf}(r_{ij})\underline{\lambda}_i \cdot \underline{\lambda}_j$, and the color electric interaction, $v_{\rm CEI}(\mathbf{r}_{ij})\underline{\lambda}_i \cdot \underline{\lambda}_j$. The $I = \lambda\sigma$ term with the color-spin operator $\underline{\lambda}_i \cdot \underline{\lambda}_j\ \sigma_i \cdot \sigma_j$ comes from the color magnetic interaction, $v_{\rm CMI}(\mathbf{r}_{ij})\underline{\lambda}_i \cdot \underline{\lambda}_j \sigma_i \cdot \sigma_j$. Their functional forms and the parameter values are the same as those used in CMA. Because of the color neutrality of Q_s-clusters, the direct terms vanish and only the exchange terms contribute to $\mathcal{E}_{\rm SQM}$:

$$X^{(\lambda)}_d = 0 \quad , \quad X^{(\lambda\sigma)}_d = 0 \quad , \quad X^{(\lambda)}_e = -48 \quad , \quad X^{(\lambda\sigma)}_e = 144 \quad . \tag{2.6}$$

The overlap integral is given as a function of

$$\begin{aligned} \boldsymbol{\rho} &\equiv \mathbf{R}_\mu + \mathbf{R}_\nu - \mathbf{R}_\sigma - \mathbf{R}_\rho; \\ \mathcal{I}^{(I)}(\boldsymbol{\rho}) &\equiv < \phi_\mu\phi_\nu \mid v^{(I)} \mid \phi_\sigma\phi_\rho > \\ &= \frac{1}{(2\pi)^{3/2}b^3} \int d\mathbf{r} \exp\left\{-\frac{1}{2b^2}\left(\mathbf{r} - \frac{\boldsymbol{\rho}}{2}\right)^2\right\} v^{(I)}(\mathbf{r}) \quad . \end{aligned} \tag{2.7}$$

In Eq.(2.4), we do not subtract the zero-point energy the center-of-mass motion of Q_s-clusters, which is $(3\hbar\omega/4)N_Q$ with $\hbar\omega \equiv \hbar^2/\bar{m}b^2$ and contributes to $\mathcal{E}_{\rm SQM}$ by $\hbar\omega/8$. This term is not essential in the infinite Q_s-matter, in contrast to the case of small N_Q.

* Eq.(2.5) in ref.3) should be read as $v_{\rm CEI}(\mathbf{r}_{ij}) = \frac{\alpha_s}{4}\left\{\frac{1}{r_{ij}} - \frac{\pi}{m_c^2}\delta(\mathbf{r}_{ij})\right\}$.

In numerical calculations, we take a simple cubic lattice of Q_s-clusters with a lattice spacing d, and focus attention on the d-dependence of $\mathcal{E}_{\rm SQM}$. In the limit of $d \to \infty$, b is to be its optimal value b_0 giving the minimum of $\mathcal{E}_{\rm SQM} = E(Q_s)/6$, where we call simply $E(Q_s)$ the internal energy of a single Q_s although it contains the zero-point energy $3\hbar\omega/4$. (In the notation of CMA, it corresponds to $\mathcal{E}_{Q_s}(\zeta = 0)$.)

For the linear confinement potential, $V_{\rm conf}(r_{ij}) = -k_1 r_{ij}$ with $k_1 = 0.18$ fm^{-2}, and the one-gluon-exchange interaction with $\alpha_s = 1.7$, we have

$$\mathcal{E}_{\rm SQM}(d \to \infty, b_0) = 1375 \text{ MeV}, b_0 = 0.91 \text{ fm} \ . \tag{2.8a}$$

For the quadratic confinement potential , $V_{\rm conf}(r_{ij}) = -k_2 r_{ij}^2$ with $k_2 = 0.15$ fm^{-3} and the one-gluon-exchange interaction with $\alpha_s = 1.7$, we have

$$\mathcal{E}_{\rm SQM}(d \to \infty, b_0) = 1488 \text{ MeV}, \quad b_0 = 0.76 \text{ fm} \ . \tag{2.8b}$$

3. Calculational procedure for Q_s-matter

In treating the Q_s-matter in a rectangular parallelepiped lattice, we apply a method developed by one of the authors (A.T.),[6] which we call "Linear-Chain Product" method and abbreriate to LCPM. At first suppose a finite lattice, where Q_s-clusters are located on the lattice sites with the lattice spacings (d_x, d_y and d_z) between neighboring clusters in the x, y, and z directions, respectively. Then

$$E(\mathbf{R}_1, \mathbf{R}_2, \cdots \mathbf{R}_{N_Q}; b) = E(d_x, d_y, d_z; b) \to E(d; b) \ , \tag{3.1}$$

where the final step is for the simple cubic lattice of $d_x = d_y = d_z = d$.

The numbers of lattice sites in the respective directions are denoted by l_x, l_y and l_z , and then $N_Q = l_x l_y l_z$. Next we label the μ-th Q_s-cluster for the vector form (m_x, m_y, m_z), by counting the sites from the some Q_s-cluster placed at the origin, and the spatial coordinate of the μ-th Q_s is given by $(m_x d_x, m_y d_y, m_z d_z)$. The ν-th Q_s is specified by (n_x, n_y, n_z).

The **B**-matrix can be given as the product of those of the respective one-dimensional cluster chain:

$$\begin{aligned} B_{\mu\nu} &= \exp\left\{\left(-\frac{1}{4b^2}\right)\left[(m_x - n_x)^2 d_x^2 + (m_y - n_y)^2 d_y^2 + (m_z - n_z)^2 d_z^2\right]\right\} \\ &\equiv B^{(x)}_{m_x,n_x} B^{(y)}_{m_y,n_y} B^{(z)}_{m_z,n_z} \ . \end{aligned} \tag{3.2}$$

We may write this in a direct product form;

$$\mathbf{B} = \mathbf{B}^{(x)} \otimes \mathbf{B}^{(y)} \otimes \mathbf{B}^{(z)} \ , \tag{3.3}$$

where each submatrix $\mathbf{B}^{(p)}$ $(p = x, y, z)$ is composed of the elements,

$$B^{(p)}_{m_p,n_p} = (s_p)^{(m_p - n_p)^2} \quad \text{with} \quad s_p \equiv \exp(-dp^2/4b^2) \ . \tag{3.4}$$

Owing to the direct product property of **B**, the inverse matrix of **B** is also of the direct product form;

$$\mathbf{B}^{-1} = (\mathbf{B}^{(x)})^{-1} \otimes (\mathbf{B}^{(y)})^{-1} \otimes (\mathbf{B}^{(z)})^{-1} \ . \tag{3.5}$$

The determinant is given in the following form;

$$\det(\mathbf{B}) = \left\{\det(\mathbf{B}^{(x)})\right\}^{l_y l_z} \left\{\det(\mathbf{B}^{(y)})\right\}^{l_x l_z} \left\{\det(\mathbf{B}^{(z)})\right\}^{l_x l_y} \tag{3.6}$$

For details of the calculational procedure for obatining $(\mathbf{B}^{(p)^{-1}})_{m_p,n_p}$ of the one-dimensional chain and taking the limit of $l_p \to \infty$, ref.6) is to be refered to. The energy per baryon can be obtained by choosing one particular Q_s as a representative and summing contributions from the other Q_s around it. By virtue of LCPM, we can calculate the expectation values of the Hamiltonian of $\overset{\text{me}}{\hat{Q}_s}$-matter in a sense that a very large number of lattice points indeed means the infinite system since the exchange effects descrease remarkably with inter-lattice distance. We can calculate the kinetic energy part and the interaction energy part, whose forms are separable in the cartesian basis such as the quadratic confinement potential and a δ-function form, in the same way as in ref.6). For the Coulomb-type potential of the color electric interaction and the linear confinement potential, however, we use the following way to calcualte their contributions to $\mathcal{I}^{(I)}(\rho)$ defined by Eq.(2.7) in the product form of the

linear chain lattice:

$$\mathcal{I}^{(+1)}(\boldsymbol{\rho}) = \sqrt{\frac{2}{\pi}} b \left\{ (1 + \frac{\rho^2}{4b^2}) \int_0^1 \exp(-\frac{\tau^2}{8b^2}\rho^2) d\tau + \exp(-\frac{\rho^2}{8b^2}) \right\} ,$$

$$\mathcal{I}^{(-1)}(\boldsymbol{\rho}) = \sqrt{\frac{2}{\pi}} \frac{1}{b} \int_0^1 \exp(-\frac{\tau^2}{8b^2}\rho^2) d\tau , \qquad (3.6)$$

where

$$\mathcal{I}^{(\pm 1)}(\boldsymbol{\rho}) = \frac{1}{(2\pi)^{3/2} b^3} \int \exp\left\{ -\frac{1}{2b^2} (\mathbf{r} - \frac{\boldsymbol{\rho}}{2})^2 \right\} \left\{ \begin{matrix} r \\ r^{-1} \end{matrix} \right\} d\mathbf{r} .$$

By integrations numerically by means of the Gaussian formula, LCPM becomes applicable.

4. Energy of the infinite Q_s-matter

For the two cases with different choice of confinement potentials (linear and quadratic), mentioned at the end of §2, the energy of the infinite Q_s-matter is calculated with a choice of a simple cubic lattice. Saturation property is shown in the next section.

1. Dependence of $\mathcal{E}_{\rm SQM}$ on lattice spacing

At first we show $\mathcal{E}_{\rm SQM}(d, b_0) = E_{\rm SQM}(d; b_0)/N_b$ and discuss the d-dependence of $\mathcal{E}_{\rm SQM}$ and those of the respective terms, when the size of Q_s is fixed to the optimum value given in Eqs.(2.8a) and (2.8b).

(a) *For linear confinement potential*

The calcualted results are shown in Fig.2(a) for this case; total energy per baryon $\mathcal{E}_{\rm SQM}(d, b_0)$ together with the respective contributions to $\mathcal{E}_{\rm SQM}$ (the kinetic energy, the color magnetic interaction (CMI), the color electric interaction (CEI), and the confinement potential). The numerical values shown near the arrows on the right ordinate are those of a single Q_s, i.e. $E(Q_s)/6$, in MeV. As d decreases, the repulsive contributions from the kinetic energy and the CMI increase, while the attractive ones from the CEI and the confinement potential become larger. As a net effect, the former overwhelms the latter, and $\mathcal{E}_{\rm SQM}(d, b_0)$ increases monotonously as d decreases.

(b) *For quadratic confinement potential*

The results for this case are shown in Fig.2(b) in the same way as in Fig.2(a). Here the contribution from the confinement potential is constant versus d. As explained in CMA the quadratic one has no effect to the inter-Q_s (mutual) energy, although it gives the large repulsive contribution to the internal energy of Q_s. The increasing repulsive contributions of the kinetic energy and the CMI overwhelm the growth of the attractive ones from the CEI, as d becomes small.

In both cases, $\mathcal{E}_{\rm SQM}(d, b_0)$ monotonously increase as the Q_s-clusters approach each other, and do not show "energy pocket", the energy minimum at a finite d. Therefore the infinite Q_s-matter has the lowest energy when the Q_s-clusters are far apart. Thus, the infinite matter limit of $\mathcal{E}_{\rm SQM}$ in this model lies on the extension of the horizontal dotted lines shown in Fig.1, as is expected.

Common features of the d-dependence of the mutual interaction energy are the following. The CEI acts attractively and the CMI repulsively, and as a result of cancellation, the net one-gluon-exchange effect is weak. The effect from the confinement potential is weakly attractive or vanishing. Therefore the mutual interaction energy comes mainly from the kinetic energy increase as d decreases, as far as the size of Q_s is fixed to the optimum value.

2. Dependence on the size of Q_s

Even if we change the spatial size of Q_s (b) from its optimum value, we can not find such energy gain from variation of both b and d as to overwhelm the loss (increase) of the internal energy of Q_s. We can see this aspoect in the examples shown in Fig.3.

3. On the direct term

The main reason of the feature mentioned above is the lack of attractive contributions from the direct term ($X_d^{(I)} = 0$ for $I = \lambda$ and $\lambda\sigma$ in Eq.(2.4)) due to the color neutrality. As shown in the studies of the nuclear saturation problem in the α-matter model[8] and of the α-like four-body correlations in light nuclei,[9] the ordinary nucleus in the ground state becomes a spatially unified system by the effect of the attractive direct term, which overwhelms the kinetic energy increase due to overlapping of the α-clusters. Such different features related to the direct term lead to sharp contrast between the SQM and the α-matter, although both are the matter composed to the $1s$-closed-shell clusters.

5. Saturation property and surface effects

In this section the saturation property of SQM is studied on the following two contexts. Firstly we discuss the effects of the boundary for the infinite matter. Secondly, treating several finite cubic lattices, we find at what baryon number the energies (per baryon) of the Q_s systems tend to $\mathcal{E}_{\rm SQM}$ ($N_b \to \infty$) given in the previous section.

When the Q_s-matter has a boundary, surface effects appear. Surface energy can be extracted from the dependence of $\mathcal{E}_{\rm SQM}$ on the position of a representative Q_s chosen for calculating $\mathcal{E}_{\rm SQM}$, that is, on the surface site, on the next deeper site, $\cdots$, and on the interior site where the saturation is realized. This is meaningful only for a given lattice spacing d (a given average baryon density $\bar{\rho}_b$), since the lowest configuration is obtained for $d \to \infty$.

In Table I the calculated results are given for several values of d corresponding to typical $\bar{\rho}_b$. There the energy of a representative Q_s in the n-th site from the surface is denoted by $\mathcal{E}(n)$, in which the self energy of the quarks (1116 MeV per baryon) is subtracted. We find that the energy is lowest for the surface Q_s and $\mathcal{E}(n)$ gradually increases with n, i.e., as the Q_s goes inward from the surface. By $n_{\rm sat}$ we denote the number n where the saturation of $\mathcal{E}(n)$ takes place. From Table I we can take $n_{\rm sat} = 3$. The d-dependence of $[\mathcal{E}(\text{surface}) - \mathcal{E}(\text{interior})]$ is shown in Figs.4(a) and 4(b) for the linear and quadratic confinement, respectively. In the Q_s-cluster model based on the constituent quark picture, the surface effects are mainly determined by the kinetic energy difference.

Surface energy can be obtained from the difference between $\mathcal{E}(n)$ and the saturated value $\mathcal{E}(\text{interior})$, which is denoted by $\Delta\mathcal{E}(n) \equiv \mathcal{E}(n) - \mathcal{E}(\text{interior})$. If we regard the surface of the cubic lattice as a part of the surface of a large sphere with a radius R, in which quarks are confined, the total energy of this system is given by

$$E_{\rm tot} = 4\pi \int_0^R \mathcal{E}(r)\bar{\rho}_b r^2 dr \quad , \tag{5.1}$$

where $\mathcal{E}(r)$ is a function made by interpolating $\mathcal{E}(n)$ at the discrete points of $R-r = (n-1)d$, and $\bar{\rho}_b = 6\times$ (density of Q_s) $=6/d^3$. Rewriting $\mathcal{E}(r)$ as $\mathcal{E}(\text{interior}) + \Delta\mathcal{E}(r)$, we have

$$E_{\rm tot} = \mathcal{E}(\text{interior})N_b + 4\pi \int_0^R \Delta\mathcal{E}(r)\bar{\rho}_b r^2 dr \quad . \tag{5.2}$$

The last term of the $r.h.s.$ is written as $4\pi\overline{\Delta\mathcal{E}}\bar{\rho}_b R^2\Delta R$, where $\overline{\Delta\mathcal{E}}R^2\Delta R \equiv \int_{R-\Delta R}^R \Delta\mathcal{E}(r)r^2dr$

and $\Delta R \equiv n_{\rm sat}d$. Using $\bar{\rho}_b R^2 = (3/4\pi)^{1/3}\bar{\rho}_b^{1/3}N_b^{2/3}$, a familar form is obtained:

$$E_{\rm tot} = \mathcal{E}(\text{interior})N_b + a_{\rm surf}N_b^{2/3} \quad , \tag{5.3}$$

with the coefficient of the surface energy term

$$a_{\rm surf} \equiv 3(8\pi)^{1/3}n_{\rm sat}\overline{\Delta\mathcal{E}} \quad . \tag{5.4}$$

For several values of $d(\bar{\rho}_b)$, $a_{\rm surf}$ are shown in Table II. In any case $a_{\rm surf}$ is negative because $\Delta\mathcal{E} < 0$. The magnitude $\mid a_{\rm surf} \mid$ increases remarkably as $\bar{\rho}_b$ increases, and becomes much larger than that of the mass formula for the nucleus ($a_{\rm surf} \simeq 17$ MeV) for $\bar{\rho}_b \gtrsim 2\rho_N (d \lesssim 2.6\text{fm})$.

Negative surface energy implies that the Q_s-matter gets energy gain when it is separated into a loose assembly of smaller parts. In other words, the multi Q_s-system is unstable againist fission. This is a direct consequence of nonexistence of "energy pocket" (energy minimum at a finite d), as shown in Fig.2.

Saturation aspects can be also seen through the N_b-dependence of $\mathcal{E}(n)$ obtained for some finite cubic lattices. We have calculated $\mathcal{E}(n)$ for $N_Q = N_b/6 = 3^3, 5^3, 7^3, 9^3$ and 199^3 and the results are shown in Fig.5 for $d = 1.8$ fm ($\bar{\rho}_b = 6\rho_N$), 2.1 fm ($\bar{\rho}_b \simeq 4\ \rho_N$) and 2.6 fm($\bar{\rho}_b = 2\ \rho_N$). We can say that at any case the energy per baryon is an increasing function of N_b and the saturation takes place completely at $N_b = 6\times 7^3 = 2058$. Its behavior depends more or less on d and b_0. For the linear confinement, the saturation takes place at $N_Q = N_b/6 = 7^3(5^3)$ for $d = 1.8$ fm ($d \geq 2.1$ fm). For the quadratic confinement, it takes place at a little less baryon number, i.e. at $N_Q = 5^3$ even for $d = 1.8$ fm. This is reasonable because the opimum size of Q_s is smaller for the quadratic confinement than for the linear one. This saturation behavior is rathe "slow", compared to the case of the nucleus, where the saturation is realized at $N_b = 4$ (the α-particle).

6. Remarks

Here we make some remarks on the results obtained in the previous sections and discuss related problems.

(1) *Energy of Q_s-matter with a given baryon density*

In the treatment of the SQM modeled in view of the Q_s-matter, it is shown that the lowest energy state of SQM is a dilute Q_s gas, namely, in the low density limit. In §5 we have considered the case when the system keeps a given average density. The cubic-lattice Q_s-matter has an average baryon density $\bar{\rho}_b = 6/d^3$, e.g., for d(fm) $\simeq 3.3 \rightarrow 2.27 \rightarrow 1.80$, $\bar{\rho}_b/\rho_N \simeq 1.0 \rightarrow 3.0 \rightarrow 6.0 (\rho_N = 0.17\ \mathrm{fm}^{-3})$. If we take the system with $\bar{\rho}_b \simeq 6.0\rho_N$, which is near the $\bar{\rho}_b$ given by the parameter set II in BMA, for example, $\mathcal{E}_{\mathrm{SQM}}(d, b_0)$ rises to 1613 MeV (238 MeV increase) for the linear confinement case and to 1702 MeV (215 MeV increase) for the quadratic confinement potential. These points are also shown in Fig.1 by the marks with the arrows on the right-end. If this value of d=1.80 fm is applied to the finite Q_s-systems treated in CMA, their energies are lifted similarly, to the d-dependence of the finite cubic lattices shown in Fig.5.

In the bag model approach, the system is confined to a single cavity. If fission of the bag is allowed, it decays into some multi-bag state like the Q_s-systems since $\mathcal{E}_{\mathrm{SQM}}$ is an increasing funciton of N_b.[4] In this case, however, the one-gluon exchange interaction plays an important role to such tendency,[4] while the kinetic energy is most influential in the cluster-model approach. In this respect too, two model approaches are complementary.

(2) *A view of strange quark systems from $N_b = 1$ to infinity*

For the constituent quark model, in CMA we have calculated the energy of the baryon (N, Λ), those of two baryons (NN and H) as well as that of Q_s. The calculated energy of the so-called H-particle is found to be close to twice the mass of the Λ-particle. For the non-strange quark systems, the compact NN systems have the energy per baryon by $200 \sim 250$ MeV higher than the nucleon mass. This is regarded as a manifestation of a core-like repulsion of the NN force in the constituent quark model.[10] In the nonstrange system, the energy increase for $N_b = 2 \rightarrow 6$ may be said as a successor of such feature of the core-like repulsion. In the u, d, s system, the color magnetic interaction (CMI) shows a particular N_b-dependence noted previously, i.e. for the flavor singlet states the CMI acts attractively for $N_b = 2$, but beyond it acts repulsively.[11] This tendency persists in the mutual interaction energy among the Q_s-clusters as N_b increases, while the color electric interaction acts

attractively. As for the mutual interaction energy, the net one-gluon-exchange contribution is small, the confinement potential effect is also weak, and thus the kinetic energy term plays a key role in this cluster-model approach.

(3) *Comparison with other hadronic strange matter*

The simplest version of the hadronic strange matter with an equal number of u, d, s quarks is the Λ matter. The attraction of $\Lambda - \Lambda$ interaction is weaker than the neutron-neutron one, and the energy per baryon of the Λ-matter is at least higher by the mass difference $m_\Lambda - m_N = 177$ MeV than the neutron matter. The $\mathcal{E}_{\mathrm{SQM}}$ of the Q_s-matter obtained here is roughly close to that of the Λ-matter at $\rho_b \simeq 6 \sim 8\ \rho_0$. This is rather close to the transition density of the Λ-matter to the uniform SQM reported earlier.[12] The H-matter (the matter composed of the H-particle like clusters) is another strange matter in a partially deconfined phase, and one of the authours (R. T.) suggested that the H-matter is possibly the lowest configuration of strange matter.[11] The energy of $\mathcal{E}_{\mathrm{SQM}}$ as the Q_s-matter is considerably higher than $\mathcal{E}_H$, since the H-state is a system which utilizes most efficiently the attractive effect from the CMI and a noncompact three-H system with a worse spatial symmetry than Q_s can avoid the inter-H repulsion.

(4) *Concerning the chemical equillibrium*

In a series of our study on the saturation property of SQM, we have restricted to the system composed of an equal number of u, d, s quarks. Because of the massives s quark, the chemical equillibrium should be imposed, in principle. For infinite matter, however, this restriction is not serious, since the one-gluon exchange interaction acts repulsively to the u, d sector but attractively to the s sector, and as a net effect an almost equal number of u, d, s appears in the chemical equillibrium.[5),13)]

In finite u, d, s systems beyond the 1s-orbital ($N_b > 6$), the situation is not simple, because the shell gap, being $\hbar\omega = 126$ (181) MeV for the linear (quadratic) confinement case, is roughly near the mass difference between s-quark and (u, d)-quark, $150 \sim 180$ MeV. Such aspects have been studied recently, although the one-gluon-exchange effect is not included.[14]

(5) *On a possible effect from the chiral field*

The conclusion of the present paper as well as the previous ones is seriously attributed to the basic assumption that all the quark-quark interaction contains the color operator $\underline{\lambda}_i \cdot \underline{\lambda}_j$. The absence of the direct term contribution from the quark-quark interaction results in the dominant repulsive effect from the kinetic energy in the mutual interaction energy among

the Q_s-clusters.

There is a room to introduce an attractive interaction between color-singlet clusters, if we consider the chiral field around them, for example, the σ-meson (neutral-scalar) like contributions. When the inter-Q_s distance d is larger or near the size of $Q_s (d \gtrsim 1.8$ fm), the σ-meson like contribution may arise in the inter-Q_s interaction through virtual excitation of Q_s-clusters due to the chiral field. If such interaction would work, the "energy pocket" in $\mathcal{E}_{\rm SQM}$ may appear for some large d where the kinetic energy increase is not so significant. This problem remains to be studied in future.

(6) *Final remark*

We have studied the saturation property of SQM in a series of works, with the motivation to study whether the notion of the absolutely stable SQM is reasonably acceptable or not. Apart from this context, to find the most favorable exsistent form of matter with large strangeness, a variety of possible configuraitons are to be studied, without restriction to simple ones such as the uniform quark matter and the Q_s-matter.

Acknowledgements

The authors would like to thank the members of Nuclear Theory Group, Department of Physics, Kyoto University for their interest in this work and helpful discussions. This work was supported by the Grant-in-Aid for Scientific Research from the Ministry of Education, Science and Culture (03804010).

REFERENCES

1. E. Witten, *Phys. Rev.***D30**(1984), 272.
   As for references on possible exotics in strongly interacting systems at early times, see those cited in ref.4).
2. For example, Proceedings of the International Workshop on Strange Quark Matter in Physics and Astrophysics (Aarhus, 1991), ed. J. Madsen and P. Haensel, *Nucl. Phys.* **B** (Proc. Suppl.) **24**(1991).
3. M. Ishii and R. Tamagaki, *Prog. Theor. Phys.* **87**(1992), 969.
4. M. Ishii and R. Tamagaki, *Prog. Theor. Phys.* **89**(1993), 657.

5. This is one of the typical cases giving rise to $\mathcal{E}_{\rm SQM}$ lower than the nucleon mass shown in: E. Farhi and R. L. Jaffe, *Phys. Rev.* **D30**(89), 2379.
6. A. Tohsaki, *Prog. Theor. Phys.* **88**(1992), 1119.
7. D. Brink, Int. Sch. of Physics, Enrico Fermi **36** (Academic Press, New York and London, 1966).
8. A. Tohsaki-Suzuki, *Prog. Theor. Phys.* **81**(1989), 370.
9. R. Tamagaki, *Prog. Theor. Phys.* **42** (1962), 748. For reviews on clusteirng aspects in light nuclei, e.g., Prog. Theor. Phys. Supplement No.52 (1972); ibid. **62** (1977); ibid. **68** (1980).
10. M. Oka and K. Yazaki, *Prog. Theor. Phys.* **66**(1981), 556, 572.
    For reviews, e.g., M. Oka and K. Yazaki, *Quarks and Nuclei*, ed. W. Weise (World Scientific, 1984), p.489. F. Myhrer and J. Wroldsen, *Rev. Mod. Phys.* **60**(1988), 629.
11. R. Tamagaki, *Prog. Theor. Phys.* **85**(1991), 321.
12. H. A. Bethe, G. E. Brown and J. Cooperstein, *Nucl. Phys.* **A462**(1987), 791.
13. R. Tamagaki and T. Tatsumi, *Prog. Theor. Phys.* Supplement No.112(1993).
14. E. P. Gilson and R. L. Jaffe, *Phys. Rev.*Lett. **71**(1993), 332.

FIGURE CAPTIONS

Fig.1. Energy per baryon versus baryon number N_b (shown in log scale), measured from the nucleon mass; $\mathcal{E} - m_N \equiv E/N_b - m_N$ in MeV. At the right end, those for infinite matter are shown. Results of a bag-model approach obtained previously[4] are shown by the filled (open) marks for u, d, s (u, d) systems; triangles, circles and squares for the bag-model parameters I, II and III used in ref.4), respectively. Results for multi-Q_s systems [3] and those of the infinite Q_s matter (this work) are shown by crosses (diamonds) connected by bold dotted lines for linear (quadratic) confinement potential. The arrows attached at the right end indicate the energy shifts as the inter-Q_s distance is changed from $d = \infty$ to 1.8 fm. Energy per baryon of ordinary nuclei and nuclear matter (N. M.) are also indicated by the open circles, just below the abscissa. Long dashed lines are only for illustration.

Fig.2. Energy per baryon of the infinite Q_s-matter $\mathcal{E}_{\rm SQM}$ versus the lattice spacing d for (a) linear confinement potential and (b) quadratic confinement potential, with the size of

Q_s shown in parenthesis. $\mathcal{E}_{\rm SQM}$ are shown by bold lines marked by *total* in scale of the left ordinate. Respective terms contributing to $\mathcal{E}_{\rm SQM}$ are also shown in the scale of the right ordinate; *kinetic* energy, color electric interaction (CEI), color manetic interaction (CMI) and confinement potential (*conf.*). The numbers shown nearby to the arrows are the values for a single Q_s in MeV.

Fig.3. Change in $\mathcal{E}_{\rm SQM}$ brought about by change of b (size of Q_s) from its optimal value b_0: (a) linear confinement potential and (b) quadratic confinement potential, for the lattice spacing indicated.

Fig.4. Difference between the energy of the Q_s-cluster located on the surface site and that on the interior site, versus the lattice distance. The bold line referes to the total energy and the thin lines to the respective contributions: (a) for the linear confinement and (b) for the quadratic confinement.

Fig.5. Change of the energy of a representative Q_s-cluster $\mathcal{E}(n)$ in finite lattices as the baryon number N_b increases as $N_Q = N_b/6 = 3^3, 5^3, 7^3, 9^3$ and 199^3. The results of the 199^3 lattice are not shown since they are the same with those of the 9^3 one. The number n of $\mathcal{E}(n)$ means the order of sites from the surface ($n = 1$) and to the inside. The results are shown for three d corresponding to the average baryon densities ($\bar{\rho}_b/\rho_N \simeq 2, 4$ and 6): (a) for the linear confinement and (b) for the quadratic confinement.

Table I. Energy (not including the quark rest-energy) of a representative Q_s, $\mathcal{E}(n)$, on the n-th site from the surface; $n = 1$ denotes the surface site and $n = \infty$ the interior one. The results for the lattice spancings d corresponding to four typical average baryon densities ($\bar{\rho}_b/\rho_N$=1, 2, 4 and 6). The respective contributions to $\mathcal{E}(n)$ are also shown. (a) for the linear confinement and (b) for the quadratic confinement.

(a) b=0.91 fm linear

d ($\bar{\rho}_b/\rho_N$) fm (−)	n	$\mathcal{E}_{\rm kin}(n)$ MeV	$\mathcal{E}_{\rm CEI}(n)$ MeV	$\mathcal{E}_{\rm CMI}(n)$ MeV	$\mathcal{E}_{\rm conf}(n)$ MeV	$\mathcal{E}(n)$ MeV
	1	478	-615	202	378	442
	2	520	-630	231	372	493
1.8 (6)	3	524	-632	234	371	497
	∞	525	-632	234	371	497
	1	387	-585	150	391	343
	2	408	-595	162	387	362
2.12 (4)	3	409	-595	163	387	363
	∞	409	-595	163	387	363
	1	319	-556	115	404	281
	2	326	-560	118	402	286
2.6 (2)	3	326	-560	118	402	286
	∞	326	-560	118	402	286
	1	289	-541	102	411	261
	2	290	-541	102	411	261
3.3 (1)	3	290	-541	102	411	261
	∞	290	-541	102	411	261

(b) b=0.76 fm quadratic

d ($\bar{\rho}_b/\rho_N$)	n	$\mathcal{E}_{\rm kin}(n)$	$\mathcal{E}_{\rm CEI}(n)$	$\mathcal{E}_{\rm CMI}(n)$	$\mathcal{E}_{\rm conf}(n)$	$\mathcal{E}(n)$
fm (−)		MeV	MeV	MeV	MeV	MeV
	1	544	-659	250	410	545
	2	572	-667	269	410	584
1.8 (6)	3	573	-668	270	410	586
	∞	574	-668	270	410	586
	1	465	-638	202	410	438
	2	476	-643	208	410	452
2.12 (4)	3	477	-643	208	410	453
	∞	477	-643	208	410	453
	1	419	-623	177	410	383
	2	422	-624	178	410	386
2.6 (2)	3	422	-624	178	410	386
	∞	422	-624	178	410	386
	1	408	-619	172	410	306
	2	408	-619	172	410	306
3.3 (1)	3	408	-619	172	410	306
	∞	408	-619	172	410	306

Table II. Change of the energy of a representative Q_s on the n-th site from the surface denoted by $n = 1$, $\Delta\mathcal{E}(n) = \mathcal{E}(n) - \mathcal{E}(\text{interior})$, for the lattice spacing d corresponding to four typical average baryon densities $\bar{\rho}_b$.

(a) $b = 0.91$ fm linear

d ($\bar{\rho}_b/\rho_N$)	$\Delta\mathcal{E}(1)$	$\Delta\mathcal{E}(2)$	$\Delta\mathcal{E}(3)$	$n_{\rm sat}\overline{\Delta\mathcal{E}}$	$a_{\rm surf}$
fm (−)	MeV	MeV	MeV	MeV	MeV
1.8 (6)	-54.8	-4.2	-0.6	-59.6	-524
2.12 (4)	-20.5	-0.9	-0.1	-21.5	-188
2.6 (2)	-4.8	-0.1	-0.0	-4.9	-43
3.3 (1)	-0.4	-0.0	-0.0	-0.4	-3.9

(b) $b = 0.76$ fm quadratic

d ($\bar{\rho}_b/\rho_N$)	$\Delta\mathcal{E}(1)$	$\Delta\mathcal{E}(2)$	$\Delta\mathcal{E}(3)$	$n_{\rm sat}\overline{\Delta\mathcal{E}}$	$a_{\rm surf}$
fm (−)	MeV	MeV	MeV	MeV	MeV
1.8 (6)	-41.0	-2.0	-0.1	-43.1	-378
2.12 (4)	-14.3	-0.2	-0.0	-14.5	-128
2.6 (2)	-2.5	-0.0	-0.0	-2.5	-22
3.3 (1)	-0.1	-0.0	-0.0	-0.1	-0.9

Fig. 1

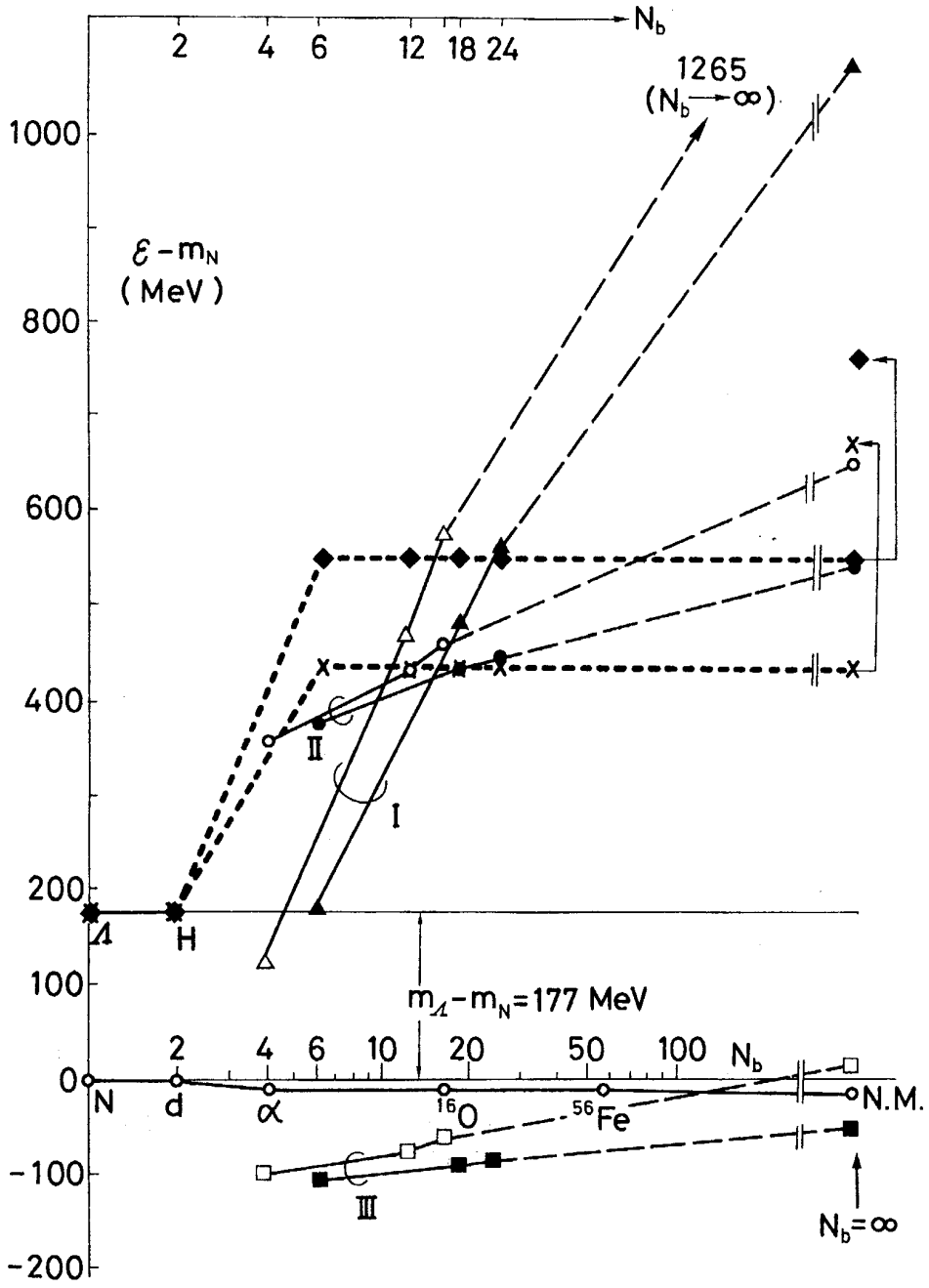
N_b
2 4 6 12 18 24
1265
(N_b → ∞)
1000
800
600
400
200
100
0
-100
-200
ε - m_N
(MeV)
Λ
H
II
I
m_Λ - m_N = 177 MeV
2 4 6 10 20 50 100 N_b
N
d
α
16O
56Fe
N.M.
III
N_b = ∞

Fig. 2(a)

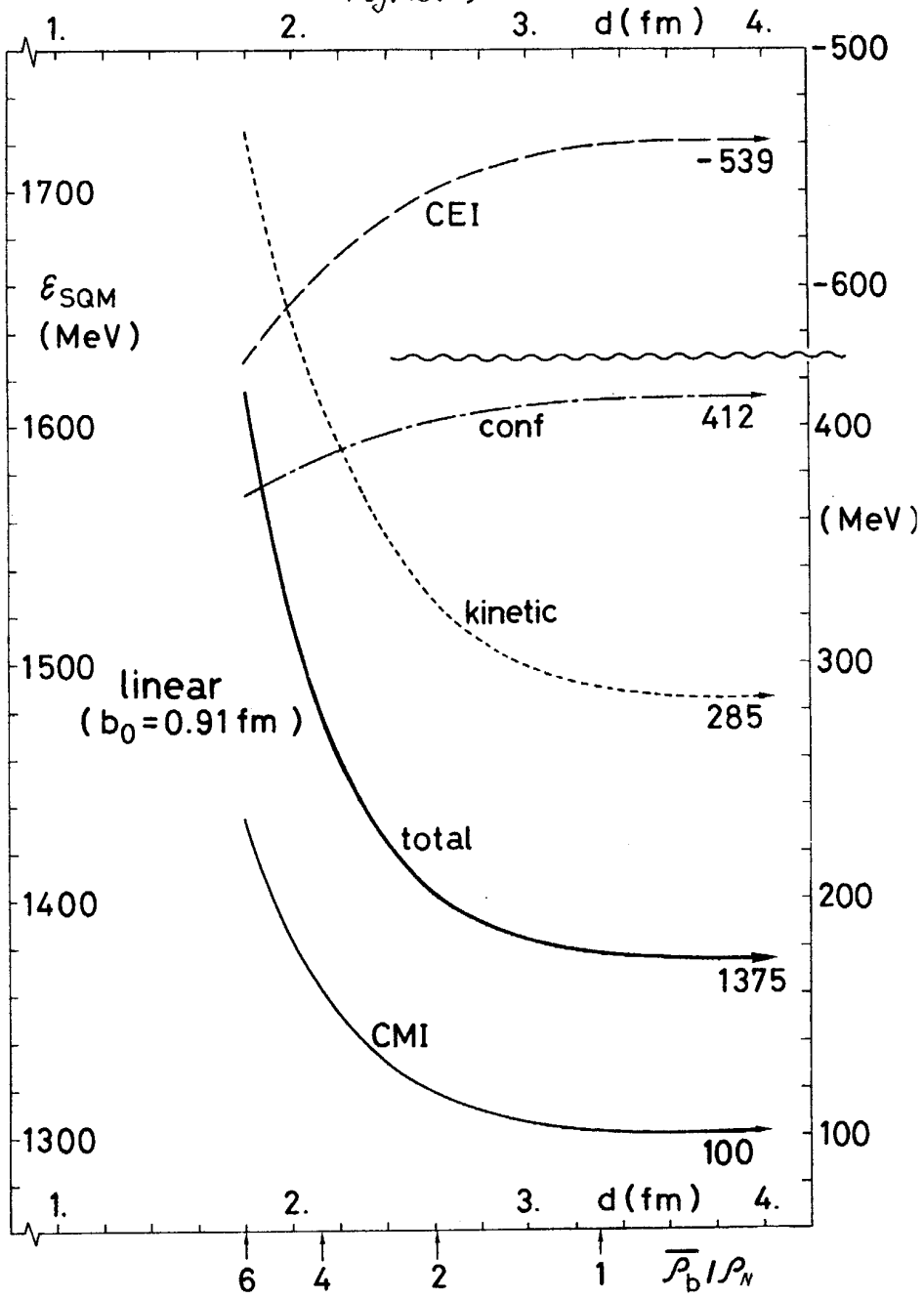
1. 2. 3. d(fm) 4.
1700
1600
1500
1400
1300
ε_SQM
(MeV)
-500
-600
400
300
200
100
(MeV)
CEI
-539
conf
412
kinetic
285
linear
(b_0 = 0.91 fm)
total
1375
CMI
100
6 4 2 1 ρ̄_b/ρ_N

Fig. 2(b)

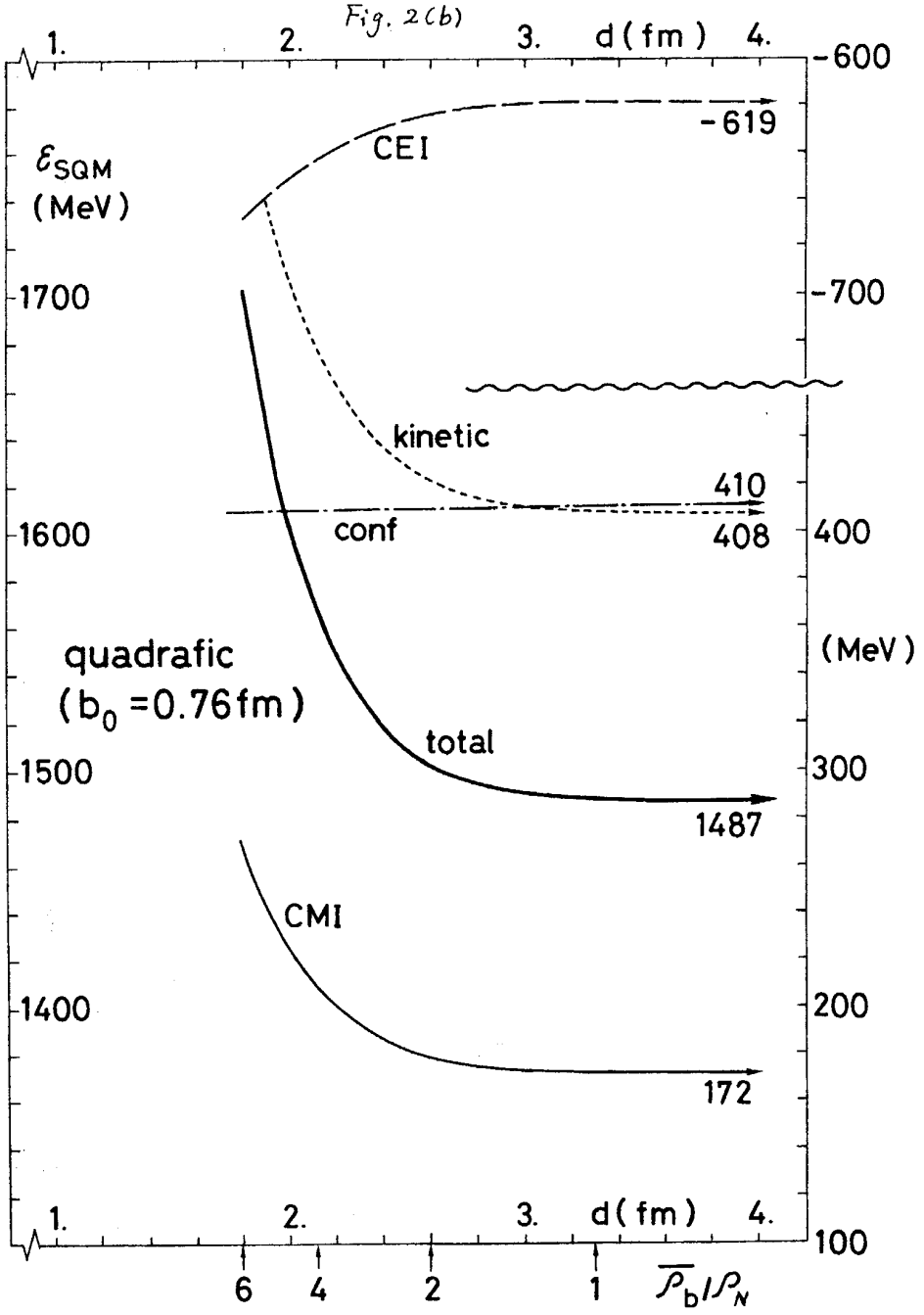
1.
2.
3.
d(fm)
4.
-600
-619
CEI
ε_{SQM}
(MeV)
1700
-700
kinetic
410
1600
conf
408
400
quadrafic
(b_0 =0.76fm)
(MeV)
total
1500
300
1487
CMI
1400
200
172
100
6
4
2
1
$\overline{\rho}_b/\rho_N$

Fig. 3(a)

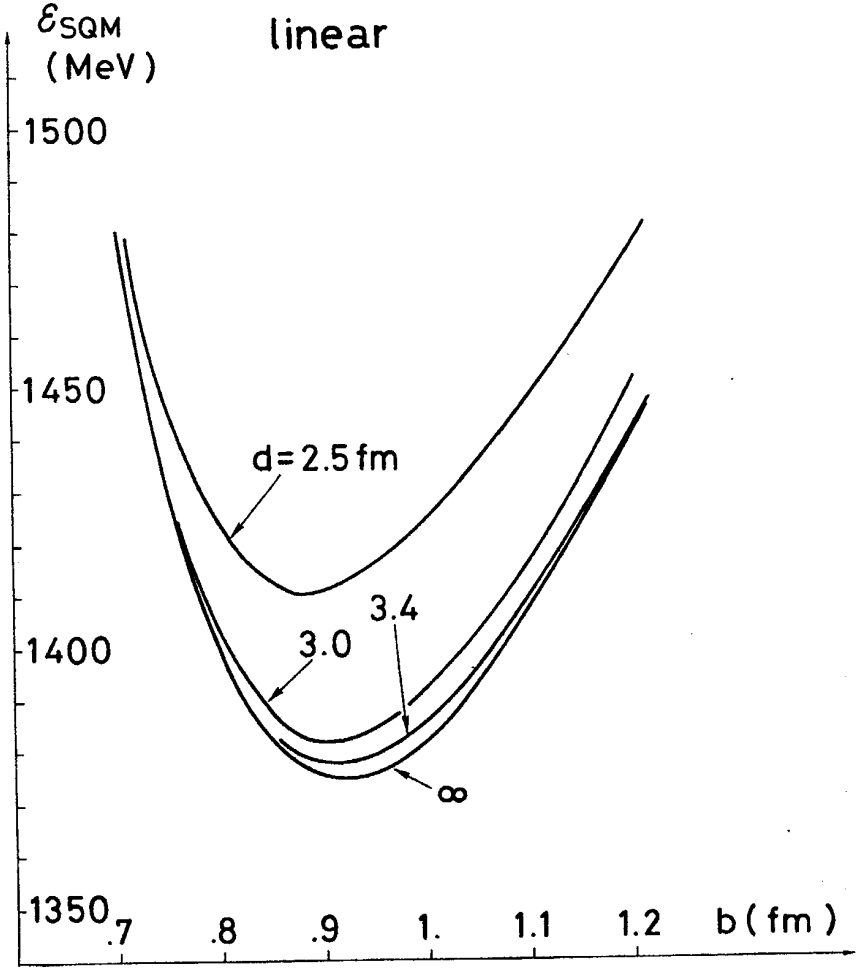
ε_{SQM}
(MeV)
linear
1500
1450
d=2.5fm
3.4
3.0
1400
∞
1350
.7
.8
.9
1.
1.1
1.2
b(fm)

Fig. 3 (b)

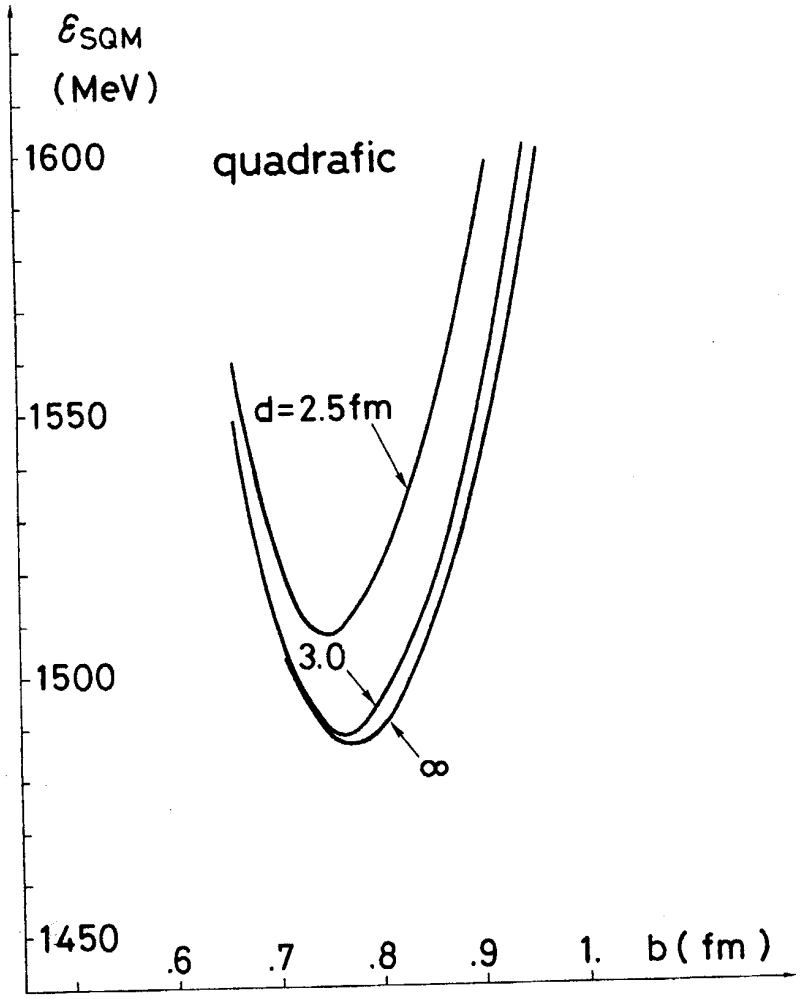
ε_{SQM}
(MeV)
1600
1550
1500
1450
quadrafic
d=2.5fm
3.0
∞
.6
.7
.8
.9
1.
b (fm)

Fig. 4(a)

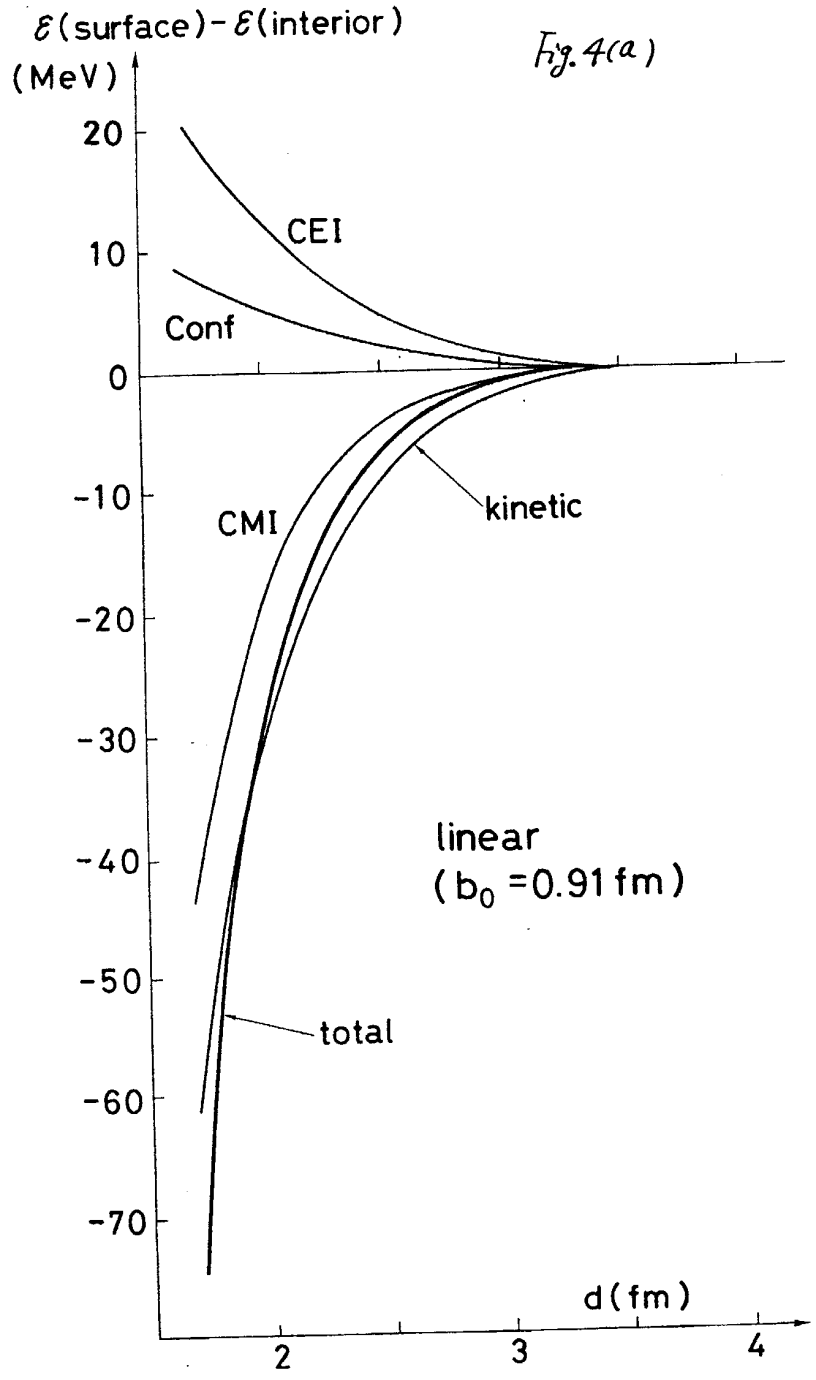
ε(surface) − ε(interior)
(MeV)
20
10
0
-10
-20
-30
-40
-50
-60
-70
CEI
Conf
CMI
kinetic
linear
(b_0 =0.91 fm)
total
d(fm)
2
3
4

Fig. 4 (b)

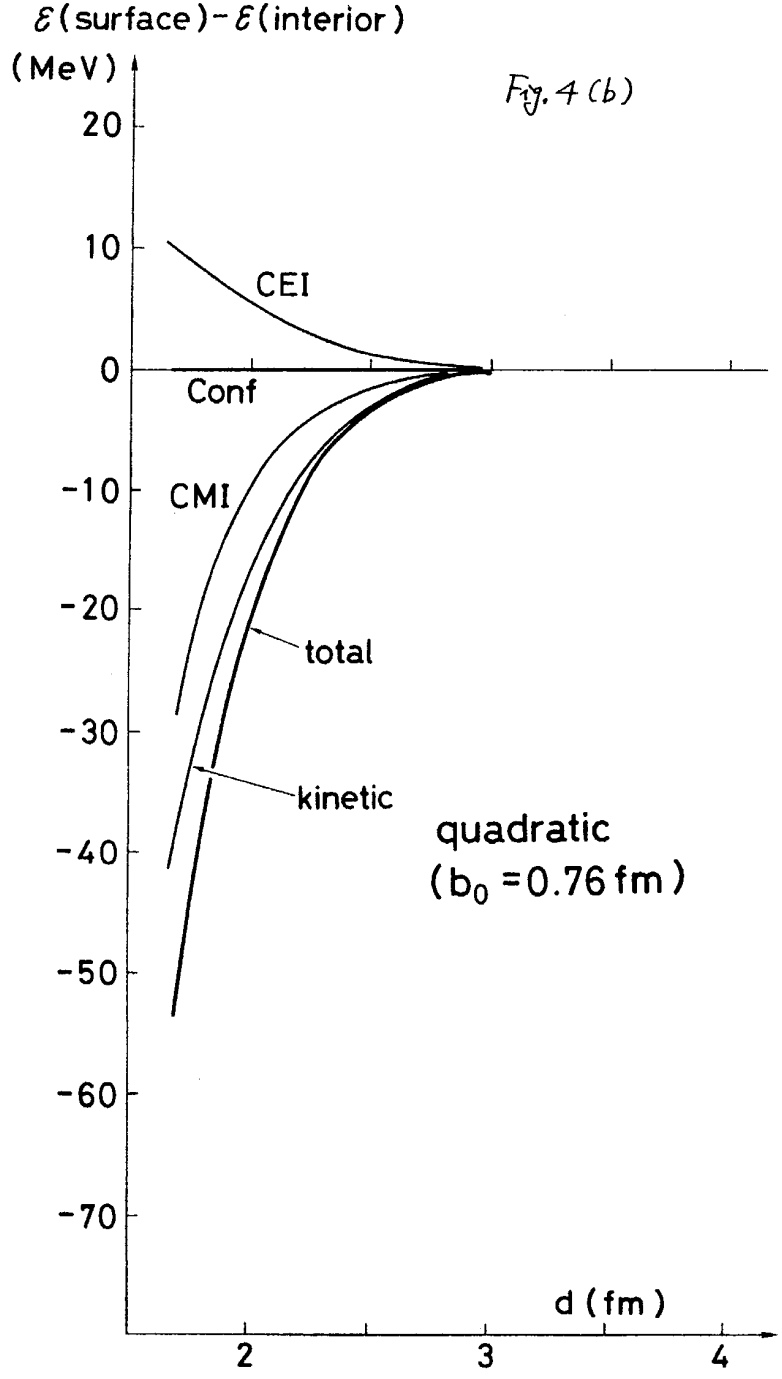
ε(surface) − ε(interior)
(MeV)
20
10
0
-10
-20
-30
-40
-50
-60
-70
CEI
Conf
CMI
total
kinetic
quadratic
(b0 = 0.76 fm)
d (fm)
2
3
4

Fig. 5

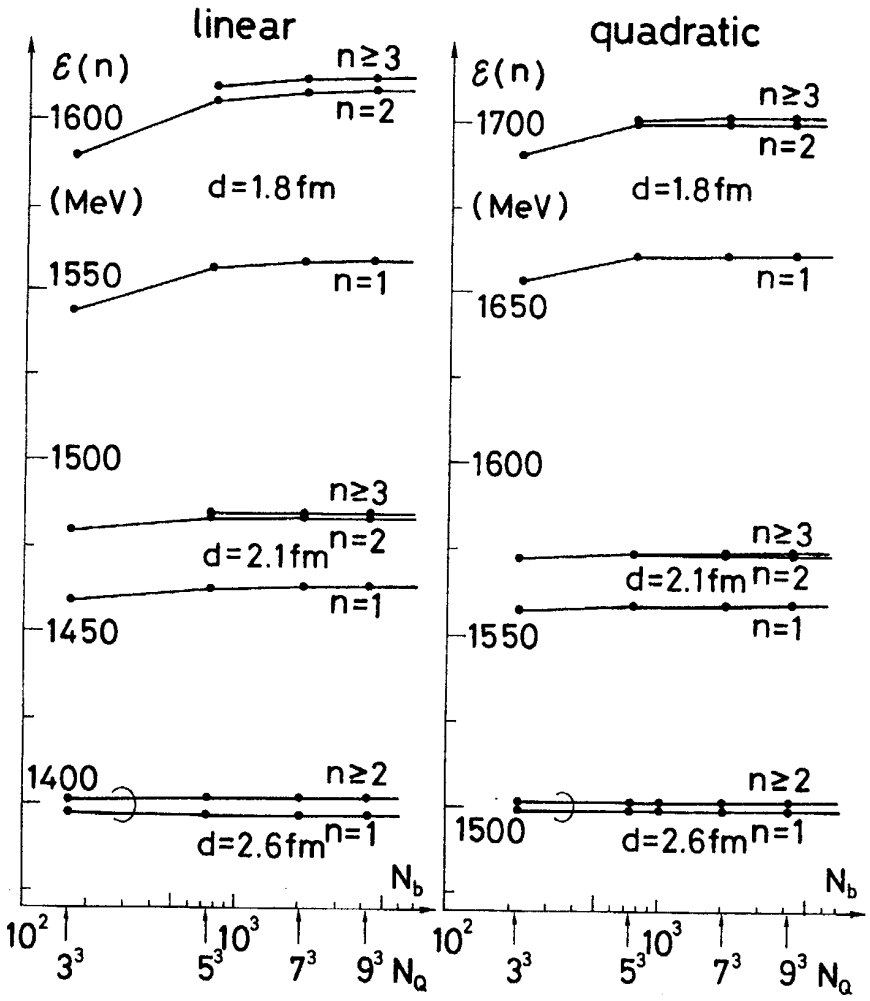
linear
quadratic
ε(n)
(MeV)
1600
1550
1500
1450
1400
1700
1650
1600
1550
1500
n≥3
n=2
n=1
n≥2
d=1.8fm
d=2.1fm
d=2.6fm
Nb
10²
3³
5³
10³
7³
9³
NQ